SUPERCONDUCTIVITY

Probing optically silent superfluid stripes in cuprates

S. Rajasekaran,[1]* J. Okamoto,[2] L. Mathey,[2] M. Fechner,[1] V. Thampy,[3] G. D. Gu,[3] A. Cavalleri[1,4]*

Unconventional superconductivity in the cuprates coexists with other types of electronic order. However, some of these orders are invisible to most experimental probes because of their symmetry. For example, the possible existence of superfluid stripes is not easily validated with linear optics, because the stripe alignment causes interlayer superconducting tunneling to vanish on average. Here we show that this frustration is removed in the nonlinear optical response. A giant terahertz third harmonic, characteristic of nonlinear Josephson tunneling, is observed in $La_{1.885}Ba_{0.115}CuO_4$ above the transition temperature T_c = 13 kelvin and up to the charge-ordering temperature T_{co} = 55 kelvin. We model these results by hypothesizing the presence of a pair density wave condensate, in which nonlinear mixing of optically silent tunneling modes drives large dipole-carrying supercurrents.

Single-layer cuprates of the type $La_{2-x-y}(Ba,Sr)_x(Nd,Eu)_yCuO_4$ exhibit an anomalous suppression of the superconducting transition temperature T_c for doping levels near 12.5% (*1*). Several studies have shown that this suppression coincides with the formation of "stripes," one-dimensional chains of charge rivers separated by regions of oppositely phased antiferromagnetism (*2*, *3*). A schematic phase diagram of $La_{2-x}Ba_xCuO_4$, adapted from (*1*), is shown in Fig. 1, along with a sketch of the stripe geometry.

Recently, high-mobility in-plane transport was found in some of these striped phases at temperatures above the bulk superconducting T_c (*4*). The existence of a striped superfluid state with a spatially oscillating superconducting order parameter, a so-called pair density wave (PDW) state, was hypothesized (*5*) to explain the anomalously low in-plane resistivity.

Superfluid stripes are difficult to detect. Scanning tunneling microscopy (STM) experiments have reported spatial modulations in the superconducting condensate strength of $Bi_2Sr_2CaCu_2O_{8+x}$ (*6*). However, STM is not sensitive to the phase of the order parameter, and these low-temperature measurements did not clarify the broader question of whether finite momentum condensation may be taking place above T_c. Also, according to the pair density wave model, superfluid transport perpendicular to the planes is frustrated owing to the stripe alignment (Fig. 1, inset). Hence, these stripes are invisible in linear *c*-axis optical measurements (*7*).

In this report, we show that superfluid stripes display characteristic signatures in the nonlinear terahertz frequency response. In $La_{1.885}Ba_{0.115}CuO_4$, we detect superfluid stripes above T_c = 13 K and up to T_{co} = 55 K.

Figure 2 displays the linear and nonlinear terahertz reflectivity spectra for two $La_{(2-x)}Ba_xCuO_4$ crystals (x = 9.5 and 15.5%), measured with single-cycle pulses (*8*) polarized along the *c* axis [see section S1 of (*9*)] and covering the spectral range between 150 GHz and 2.5 THz [see section S2 of (*9*)]. At these doping levels, the material exhibits homogeneous superconductivity and only weak stripe order, with transition temperatures of $T_{co} \sim T_c$ = 34 K (x = 9.5%) and $T_{co} \sim$ 40 K > T_c = 32 K (x = 15.5%).

The low-temperature linear reflectivities (T = 5 K < T_c), show Josephson plasma edges at ω_{JP0} = 500 GHz and ω_{JP0} = 1.4 THz for x = 9.5 and 15.5%, respectively (see dashed curves in Fig. 2, A and C). The reflectivity edges shifted to lower frequencies with increasing temperature, indicating a decrease in superfluid density [Fig. 2, B and D, and section S2 of (*9*)].

Nonlinear reflectivities, measured at field strengths between 20 and 80 kV/cm (see Fig. 2, A and C) displayed two characteristic effects of nonlinear interlayer Josephson coupling: (i) a field-dependent red shift of the plasma edge (*10*–*12*) and (ii) a reflectivity peak at the third harmonic of the pump field $\omega \approx 3\omega_{pump}$ (*13*). The third-harmonic field amplitude $E(3\omega_{pump})$ scaled with the cube of the incident field strength $E(\omega_{pump})$ (Fig. 2E), decreased in strength with temperature, and disappeared for $T = T_c$, tracking the superfluid density $\omega\sigma_2(\omega\rightarrow 0)$ (see Fig. 2, C, D, and F).

These observations are well understood by a semiquantitative analysis of the interlayer phase dynamics of a homogeneous layered superconductor (*10*, *12*, *14*). For a *c*-axis electric field $E(t) = E_0\sin(\omega_{pump}t)$ the interlayer phase difference $\theta(t)$ advances in time, t, according to the second Josephson equation $\frac{\partial\theta(t)}{\partial t} = \frac{2edE(t)}{\hbar}$, where d is the interlayer spacing (~1 nm), $2e$ is the Cooper pair charge, and $\hbar$ is Planck's constant h divided by 2π (*15*). Because the *c*-axis superfluid density ρ_c scales with the order parameter phase difference $\rho_c \propto \cos\theta$ and because $\rho_c \propto \omega_J^2$, the plasma frequency renormalizes as $\omega_J^2 = \omega_{JP0}^2\cos(\theta) = \omega_{JP0}^2\cos[\theta_0\cos(\omega_{pump}t)] \approx \omega_{JP0}^2\left[1-\frac{\theta_0^2}{4}-\frac{\theta_0^2\cos(2\omega_{pump}t)}{4}\right]$, where $\theta_0 = 2edE_0/\hbar\omega_{pump}$, an average red shift of the equilibrium plasma resonance ω_{JP0} is hence estimated as $\omega_J^2 = \omega_{JP0}^2\left(1-\frac{\theta_0^2}{4}\right)$. Secondly, a tunneling supercurrent, I, is excited at the first and third harmonic of the driving field, $I(t) = I_c\sin[\theta_0\cos(\omega_{pump}t)] \approx I_c\left[\theta_0\cos(\omega_{pump}t) - \frac{\theta_0^3}{6}\cos^3(\omega_{pump}t)\right]$, giving rise to third harmonic radiation. Finally, because the third-harmonic signal is proportional to I_c, it is expected to follow the same temperature dependence as the superfluid density.

More comprehensive numerical simulations, based on space (x, not to be confused with the symbol for doping concentration)– and time (t)–dependent one-dimensional sine-Gordon equation for the Josephson phase $\theta(x,t)$ [see section S3 of (*9*)] (*12*, *14*, *16*, *17*), were used to obtain the electromagnetic field at the surface of the superconductor and to calculate the reflectivity for arbitrary field strengths. These simulations, reported in Fig. 3, reproduce the experimental data closely.

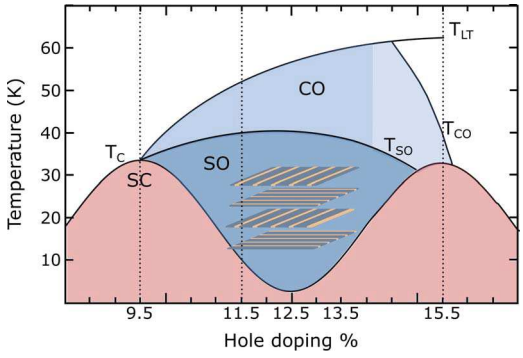

Fig. 1. Phase diagram for $La_{2-x}Ba_xCuO_4$. SC, SO, and CO denote the bulk superconducting, spin- and charge-ordered (striped), and charge-only–ordered phases, respectively. T_c, T_{so}, and T_{co} are the corresponding ordering temperatures. T_{LT} denotes the orthorhombic-to-tetragonal structural transition temperature. The samples examined in this study are x = 9.5, 11.5, and 15.5% (dotted lines). Further, a schematic stripe-ordered state is shown wherein the tan stripes depict the charge rivers and the gray stripes depict the antiferromagnetic insulating region (inset). Figure adapted with permission from (*1*).

[1]Max Planck Institute for the Structure and Dynamics of Matter, Hamburg, Germany. [2]Centre for Optical Quantum Technologies and Institute for Laser Physics, University of Hamburg, Hamburg, Germany. [3]Condensed Matter Physics and Materials Science Department, Brookhaven National Laboratory, Upton, 11973 NY, USA. [4]Clarendon Laboratory, Department of Physics, University of Oxford, Oxford, UK.
*Corresponding author. Email: andrea.cavalleri@mpsd.mpg.de (A.C.); srivats.rajasekaran@mpsd.mpg.de (S.R.)

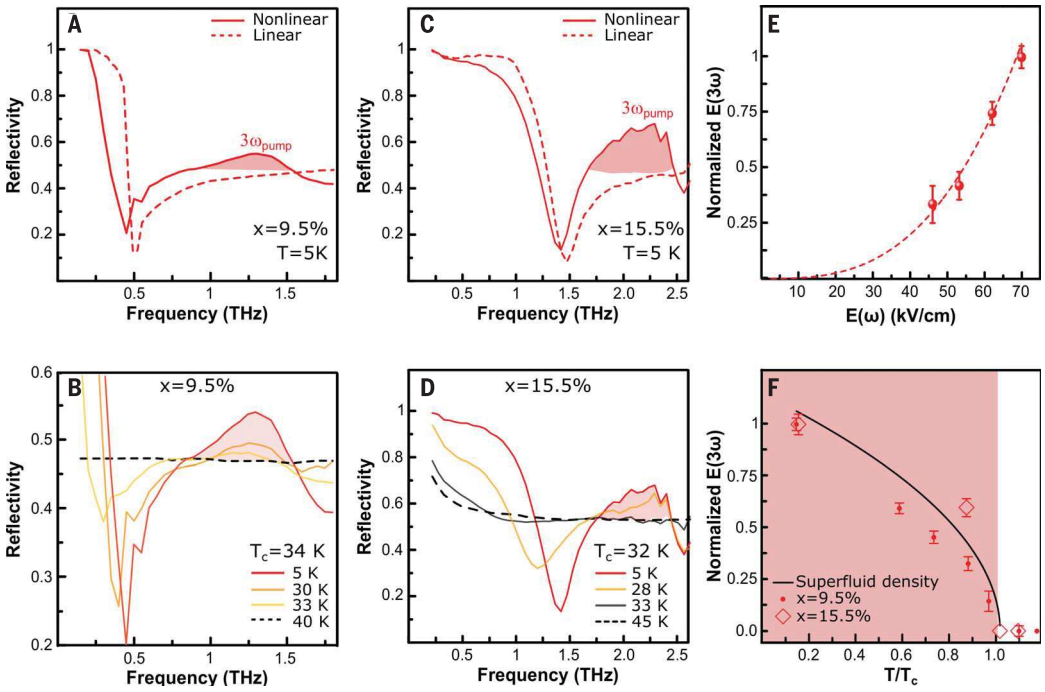

Fig. 2. Third harmonic from homogeneous superconductor. (**A**) Linear and nonlinear reflectivity of $La_{2-x}Ba_xCuO_4$, where x = 9.5%, measured at T = 5 K with ω_{pump} = 450 GHz. The linear reflectivity displays a Josephson plasma edge at ω_{JP0} = 500 GHz (0.5 THz), whereas the nonlinear reflectivity shows a red shift of the edge and third-harmonic generation (red shading). (**B**) Temperature dependence of nonlinear reflectivity for x = 9.5%. The third-harmonic peak disappears above T_c = 34 K. (**C**) Linear and nonlinear reflectivity for x = 15.5%, measured with ω_{pump} = 700 GHz. (**D**) Temperature dependence of third-harmonic generation in x = 15.5%. Third-harmonic generation (red shading) disappears above T_c = 32 K. (**E**) Third-harmonic electric field strength (normalized to the highest signal) plotted as a function of the incident electric field strength [definition explained in section S1 of (*9*)] measured at T = 5 K from the x = 9.5% sample. The third-harmonic field displays a cubic dependence on the incident field strength. (**F**) Temperature dependence of the third-harmonic amplitude (normalized to the measurement at T = 5 K) from the x = 9.5 and 15.5% doping. The superfluid density [$(\omega\sigma_2(\sigma\rightarrow 0)]$ (normalized to the measurement at T = 5 K) extracted from the linear optical properties of the x = 9.5% sample is also shown. All of the quantities vanish above T_c. Red shading indicates the bulk superconducting phase.

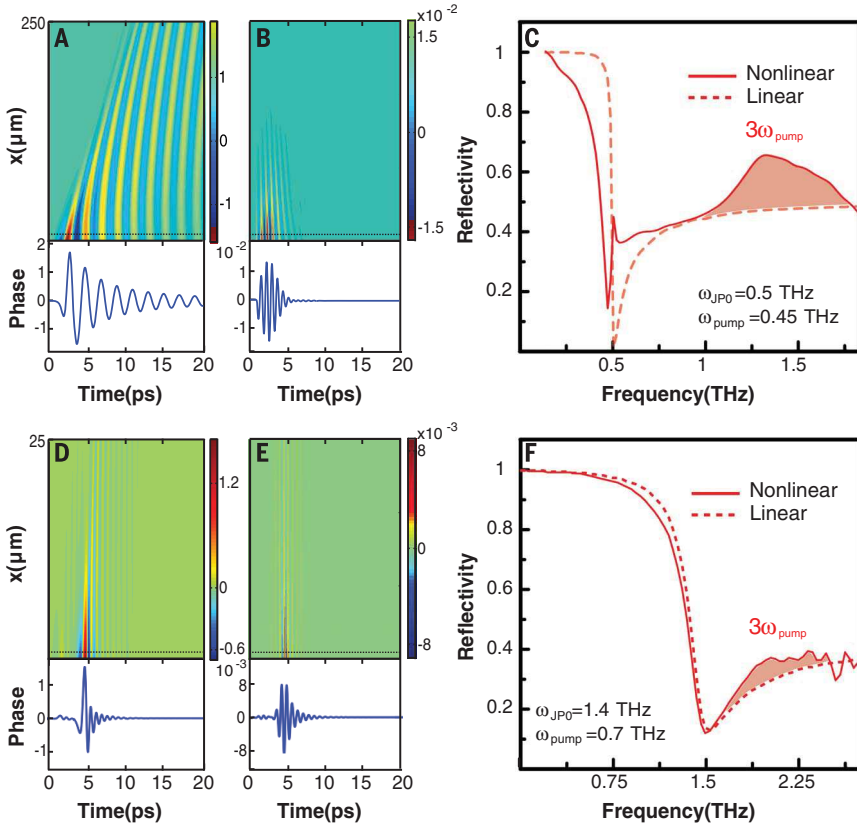

Fig. 3. Simulated nonlinear reflectivity for homogeneous superconductivity. Simulations at x = 9.5 and 15.5% doping. (**A**) Simulated space (x, not to be confused with the symbol for doping concentration)– and time (t)–dependent order parameter phase [$\theta(x, t)$] obtained by numerically solving the sine-Gordon equation on x = 9.5% samples [see section S3 of (*9*)]. The equation makes use of equilibrium superfluid density extracted from the linear optical properties and assumes excitation with terahertz pulses of shape and strength used in the experiment. The horizontal dotted lines indicate the spatial coordinate x at which the line cuts are displayed (lower panel). (**B**) Simulated order parameter phase (A) after frequency filtering centered at $3\omega_{pump}$ with its corresponding line cut (lower panel). (**C**) Simulated reflectivity in the linear (E = 0.1 kV/cm) and the nonlinear (E = 80 kV/cm) regime. The third-harmonic generation component is highlighted (red shading). (**D** to **F**) Same as in (A) to (C) but for x = 15.5%.

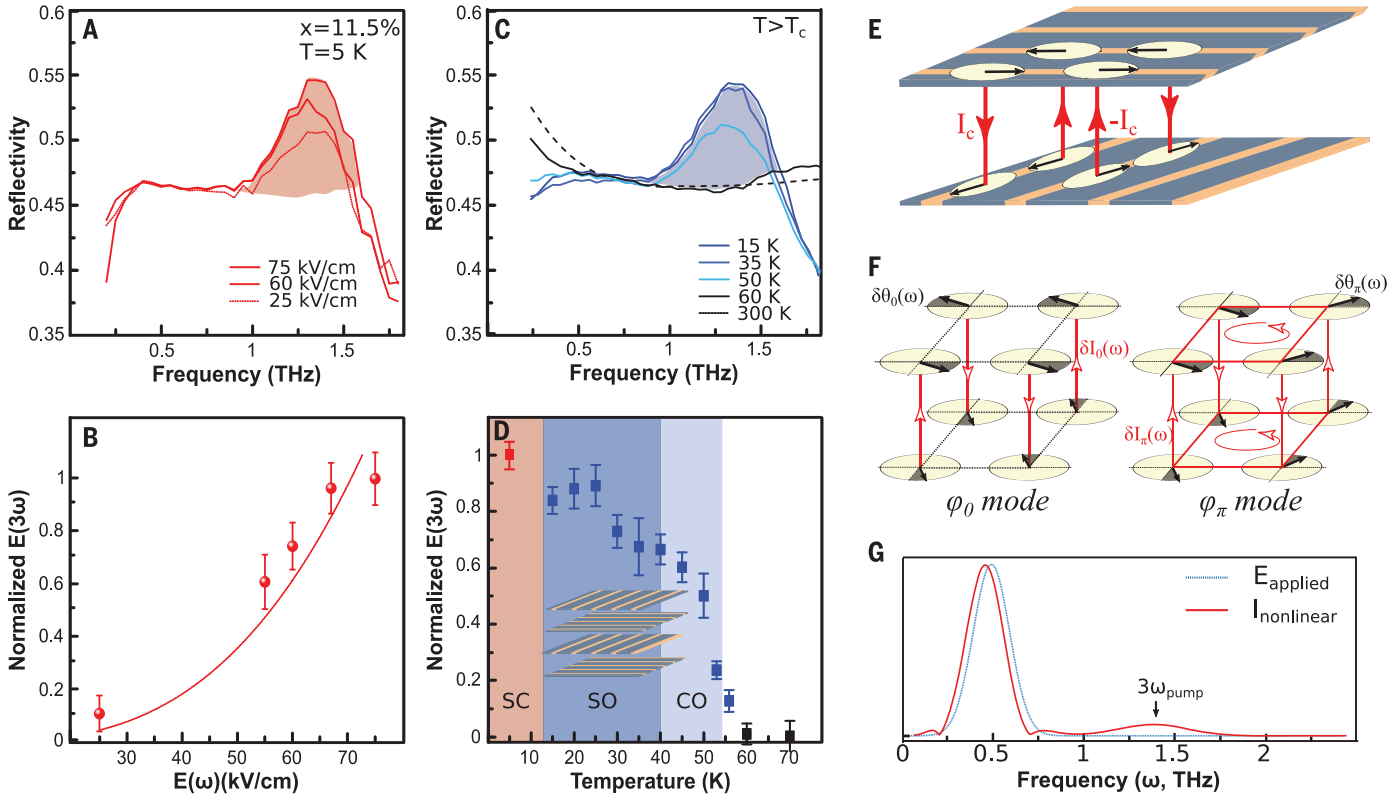

Fig. 4. Third-harmonic generation in the striped phase. (**A**) Nonlinear frequency-dependent reflectivity measured in the striped $x = 11.5\%$ samples recorded for three different field strengths at $T = 5$ K ($< T_c = 13$ K). (**B**) Electric field dependence of the third-harmonic amplitude for $T = 5$ K. (**C**) Temperature dependence of the nonlinear reflectivity for $T > T_c = 13$ K. (**D**) Temperature dependence of the third-harmonic signal (normalized to the highest field measurements at $T = 5$ K). (**E**) Schematic of the order parameter phase in a pair density wave condensate. The black arrows represent the superconducting order parameter phase at each lattice point. Interlayer tunneling from perpendicularly aligned superfluid stripes is equivalent to a checkerboard lattice of alternating $\pi/2$ and $-\pi/2$ phase Josephson junctions. Such a lattice has tunneling currents of I_c and $-I_c$ flowing at the neighboring junctions at equilibrium (thick red lines). (**F**) Excitation modes of the PDW indicating the φ_0 and φ_π modes (see text). The shaded region under the black arrow represents the phase excursion from the equilibrium geometry ($\delta\theta_0$ and $\delta\theta_\pi$). Corresponding current fluctuations δI_0 and δI_π produced by such excitations are also depicted (thin red lines). (**G**) Calculated nonlinear current response for the unit cell of (E) after application of a single-cycle optical pulse centered at 500 GHz frequency [see section S5 of (*9*) for details].

We next turn to the key results of this report, which provide evidence for superfluidity in the normal-state striped phase in $La_{1.885}Ba_{0.115}CuO_4$ ($x = 11.5\%$). In this compound, striped charge order coexists with superconductivity below $T_c = 13$ K and extends into the normal state up to $T_{co} = 55$ K (*1*).

Figure 4A displays the results for $T < T_c = 13$ K. Note that in this material, the equilibrium Josephson plasma resonance was at lower frequency than in the other two compounds with higher T_c (at ~150 GHz) and could not be observed [see section S2 of (*9*)]. However, a third harmonic at $\omega = 3\omega_{pump} \approx 1.4$ THz was clearly observed. Notably, the third-harmonic signal remained finite also for $T > T_c = 13$ K and up to $T \sim T_{co} = 55$ K (Fig. 4, C and D). A giant third harmonic, amounting to several percent of the driving field, can be understood only in the presence of superconducting tunneling above T_c and up to T_{co}.

In the following paragraphs, we show that a pair density wave, which does not show features of superfluidity in the linear optical properties, retains the large nonlinear optical signal of the homogeneous condensate. As shown in Fig. 4E, the order parameter phase of the PDW, encoded by the vector angle (black arrow), changes between neighboring stripes and rotates by 90° from one plane to the next (*18*), resulting in a checkerboard lattice of $\pi/2$ and $-\pi/2$ Josephson junctions. Hence, the equilibrium PDW supports a lattice of staggered tunneling supercurrents, which average out to zero (thick red arrows in Fig. 4E).

The interlayer phase fluctuations probed in the optical response are described by two normal modes, termed here φ_0 and φ_π. The φ_0 mode is optically active. For an optical field $E(t) = E_0\sin(\omega_{pump}t)$, one has identical phase excursions $\delta\theta_0(t) = \frac{2edE_0}{\hbar\omega_{pump}}\cos(\omega_{pump}t)$ at each site (shading under black arrows in Fig. 4F). However, current fluctuations $\delta I_0(t)$ of equal magnitude, but opposite sign, at neighboring $\pi/2$ and $-\pi/2$ junctions, makes this mode silent (red arrows in Fig. 4F). The second φ_π mode consists of phase excursions $\delta\theta_\pi(t)$ occurring in opposite directions at neighboring sites and is optically inactive (see Fig. 4F).

In the nonlinear regime, the optical response of the PDW is no longer zero. Because φ_0 is odd and φ_π is even, a nonlinear expansion of the Josephson energy (U) can be written as $U(\varphi_0,\varphi_\pi) \propto J_0{\varphi_\pi}^2 - J''\varphi_\pi + C{\varphi_0}^2\varphi_\pi$, where J_0 and J'' are the in-plane and out-of-plane Josephson energies and $C = J''/2$, with $J_0 \gg J''$, where C is the coupling constant between the two normal modes [see section S5 of (*9*)].

A large third-harmonic signal is readily predicted from the ${\varphi_0}^2\varphi_\pi$ coupling term. For an optical field of the type $E(t) = E_0\sin(\omega_{pump}t)$, which acts only on the mode φ_0, the equations of motion of the phase are $\varphi_0 \approx \omega_{pump}E_0\cos(\omega_{pump}t)$ and $\varphi_\pi \approx -2C{\varphi_0}^2$. These coupled equations imply not only phase oscillations in φ_0 mode at ω_{pump}, i.e., $\delta\theta_0(\omega_{pump})$, but also indirect excitation of the optically inactive φ_π mode. Because in the equation of motion for φ_π the driving force is proportional to ${\varphi_0}^2$, the phase of this mode $\delta\theta_\pi$ is driven at $2\omega_{pump}$. Because the total nonlinear current $I_{tot} = \Sigma I_{junctions}$ contains terms of the type $I^*_{tot} \sim 2I_c\varphi_0\varphi_\pi$, the two phase coordinates $\varphi_0(\omega_{pump})$ and $\varphi_\pi(2\omega_{pump})$ are mixed

and produce current oscillations at the difference and sum frequencies ω_{pump} and $3\omega_{pump}$. A numerical solution of the two equations of motion with realistic parameters for the Josephson coupling energies J_0 and J'' displays oscillatory currents at the fundamental and third harmonic [Fig. 4G, also see section S5 of (*9*) for details on the simulations].

Finally, from the model above, the third-harmonic current is predicted to scale linearly with the out-of-plane critical current and, hence, the superfluid density of the stripes. From the plot in Fig. 4D, the local superfluid density at spin- and charge-ordering temperature T_{so} is found to be 60% of that measured below T_c and subsequently decreases continuously as the temperature is increased further, before vanishing at T_{co}.

Although the model discussed above provides a plausible description of the experimental observations, other hypotheses for the origin of the third-harmonic signal for $T > T_c$ should be considered. The measured and simulated third harmonic is far larger than, and hence easily distinguished from, the effect of noncondensed quasiparticles. The nonlinear susceptibility detected in the present experiments $\chi^{(3)} \sim 10^{-15} m^2/V^2$ (obtained from the electric field strengths at the fundamental and third harmonic) is several orders of magnitude bigger than typical cubic nonlinearities ($\chi^{(3)} \sim 10^{-18} - 10^{-20} m^2/V^2$) (*19*–*21*). Furthermore, first-principle calculations show that, for this compound, the value of $\chi^{(3)}$ from quasiparticle transport within anharmonic bands is at least three orders of magnitude smaller than what is measured here [see section S6 of (*9*)].

A second alternative may involve the sliding of a charge density wave along the *c* axis, as discussed in (*22*) for blue bronze. However, the efficiency of the sliding of a charge density wave, reported in (*22*) for kilohertz frequency excitation, is expected to reduce strongly at higher excitation frequencies and can be ruled out for the terahertz irradiation [see section S7 of (*9*)]. The results for the 15.5% sample, where the third-harmonic signal disappears at $T_c = 32$ K ($< T_{co} =$ 40 K), further indicate that the third harmonic results from superconducting tunneling rather than charge ordering.

The observation of a colossal third-harmonic signal in the stripe-ordered state of $La_{1.885}Sr_{0.115}CuO_4$ provides compelling experimental evidence for finite momentum condensation in the normal state of cuprates and underscores the power of nonlinear terahertz optics as a sensitive probe of frustrated excitations in quantum solids. A natural direction for this line of research involves the study of other forms of charge order that compete or coexist with superconductivity, such as those found in $YBa_2Cu_3O_{6+x}$ (*23*, *24*). One may also find application of these techniques in other regimes of the cuprate pseudogap, with finite superfluid density, with vanishing range phase correlations (*25*, *26*), or where other forms of density waves (*27*, *28*) have been discussed.

REFERENCES AND NOTES

1. M. Hücker *et al*., *Phys. Rev. B* **83**, 104506 (2011).
2. P. Abbamonte *et al*., *Nat. Phys.* **1**, 155–158 (2005).
3. J. M. Tranquada, B. J. Sternlieb, J. D. Axe, Y. Nakamura, S. Uchida, *Nature* **375**, 561–563 (1995).
4. Q. Li, M. Hücker, G. D. Gu, A. M. Tsvelik, J. M. Tranquada, *Phys. Rev. Lett.* **99**, 067001 (2007).
5. E. Berg *et al*., *Phys. Rev. Lett.* **99**, 127003 (2007).
6. M. H. Hamidian *et al*., *Nature* **532**, 343–347 (2016).
7. C. C. Homes *et al*., *Phys. Rev. B* **85**, 134510 (2012).
8. J. Hebling, K.-L. Yeh, M. C. Hoffmann, B. Bartal, K. A. Nelson, *J. Opt. Soc. Am. B* **25**, B6 (2008).
9. Materials and methods are available as supplementary materials.
10. Y. Laplace, A. Cavalleri, *Adv. Phys. X* **1**, 387–411 (2016).
11. A. Dienst *et al*., *Nat. Photonics* **5**, 485–488 (2011).
12. A. Dienst *et al*., *Nat. Mater.* **12**, 535–541 (2013).
13. (1) In addition to the two features, a reflectivity spike at ω_{JP0} is observed for $x = 9.5\%$ doping. This feature corresponds to a parametric amplification of the Josephson plasma waves [see (*14*)]. (2) The central frequency of the terahertz pulses for experiments in $x = 9.5$ and 11.5% was $\omega_{pump} = 0.45$ THz. Note that to obtain a clear third-harmonic signal without interference from the reflectivity edge at the plasma frequency in $x = 15.5\%$ sample, terahertz pulses with $\omega_{pump} = 0.7$ THz were used.
14. S. Rajasekaran *et al*., *Nat. Phys.* **12**, 1012–1016 (2016).
15. B. D. Josephson, *Rev. Mod. Phys.* **36**, 216–220 (1964).
16. S. Savel'ev, V. A. Yampol'skii, A. L. Rakhmanov, F. Nori, *Rep. Prog. Phys.* **73**, 026501 (2010).
17. X. Hu, S.-Z. Lin, *Supercond. Sci. Technol.* **23**, 053001 (2010).
18. E. Berg, E. Fradkin, S. A. Kivelson, J. M. Tranquada, *New J. Phys.* **11**, 115004 (2009).
19. R. W. Boyd, Z. Shi, I. De Leon, *Opt. Commun.* **326**, 74–79 (2014).
20. B. Buchalter, G. R. Meredith, *Appl. Opt.* **21**, 3221–3224 (1982).
21. O. Schubert *et al*., *Nat. Photonics* **8**, 119–123 (2014).
22. T. Chen, L. Mihály, G. Grüner, *Phys. Rev. B Condens. Matter* **36**, 2931–2934 (1987).
23. G. Ghiringhelli *et al*., *Science* **337**, 821–825 (2012).
24. J. Chang *et al*., *Nat. Phys.* **8**, 871–876 (2012).
25. J. Corson, R. Mallozzi, J. Orenstein, J. N. Eckstein, I. Bozovic, *Nature* **398**, 221–223 (1999).
26. L. S. Bilbro *et al*., *Nat. Phys.* **7**, 298–302 (2011).
27. K. Fujita *et al*., *Proc. Natl. Acad. Sci. U.S.A.* **111**, E3026–E3032 (2014).
28. P. A. Lee, *Phys. Rev. X* **4**, 031017 (2014).

ACKNOWLEDGMENTS

We thank S. A. Kivelson and J. M. Tranquada for helpful feedback on the manuscript. We thank D. Nicoletti for providing us with the linear reflectivity data of the $x = 11.5\%$ sample. The research leading to these results received funding from the European Research Council under the European Union's Seventh Framework Programme (FP7/2007-2013) and ERC grant agreement no. 319286 [Frontiers in Quantum Materials' Control (Q-MAC)]. Work performed at Brookhaven was supported by the U.S. Department of Energy, Division of Materials Science under contract no. DE-AC02-98CH10886. The data from the terahertz measurements and the simulations are kept at the Cavalleri Laboratory at Max Planck Institute of Structure and Dynamics, Hamburg, and are available from the authors upon request.

SUPPLEMENTARY MATERIALS

www.sciencemag.org/content/359/6375/575/suppl/DC1
Materials and Methods
Figs. S1 to S8
References (*29*–*34*)

30 March 2017; accepted 22 December 2017
10.1126/science.aan3438

Science

Probing optically silent superfluid stripes in cuprates

S. Rajasekaran, J. Okamoto, L. Mathey, M. Fechner, V. Thampy, G. D. Gu and A. Cavalleri

Science **359** (6375), 575-579.
DOI: 10.1126/science.aan3438

A nonlinear peek into stripes

In many theoretical models of high-temperature superconductors, remnants of superconductivity persist to temperatures higher than the transition temperature, T_C. Rajasekaran *et al.* used nonlinear terahertz spectroscopy to probe this region of the phase diagram of a cuprate superconductor that is well known for a stripe phase that appears for certain doping levels (see the Perspective by Ergeçen and Gedik). For a sample deep in the stripe phase, a large nonlinear signal persisted from the superconducting region up to temperatures much higher than T_C. The findings suggest the formation of a peculiar spatially modulated superconducting state called the pair-density wave.

Science, this issue p. 575; see also p. 519